An ODE-Enabled Distributed Transient Stability Analysis for Networked Microgrids

Yifan Zhou, Peng Zhang, *Senior Member, IEEE* and Meng Yue, *Member, IEEE*

***Abstract*—Networked microgrid (NMG) exhibits noteworthy resiliency and flexibility benefits for the mutual support from neighboring microgrids. With high penetration of distributed energy resources (DERs) and the associated controls, the transient stability analysis of NMGs is of critical significance. To address the issues of computation burdens and privacy in the centralized transient analysis, this paper devises an ordinary differential equation (ODE)-enabled distributed transient stability (DTS) methodology for NMGs. First, an ODE-based microgrid model is established to capture the dynamics in the droop control of DERs as well as network and load. Further, a distributed DTS is devised for the ODE representation of an NMG, allowing a privacy-preserving transient analysis of each microgrid while accurately reconstructing the frequency dynamics under droop controls in all DERs. Extensive tests are performed to verify the validity of the ODE-based microgrid model through both dynamic response and eigenvalue analysis, and the efficacy of the DTS algorithm in simulating the large signal responses and the frequent fluctuations in NMG.**

***Index Terms*—Networked microgrids, distributed transient stability analysis, ordinary differential equations, droop control.**

I. Introduction

Microgrids (MGs) have received major attentions for its flexibility in operation and accommodating the renewable energy [1]. A networked microgrid (NMG) system incorporating multiple neighboring microgrids has shown a great potential to harness resiliency benefits by leveraging the mutual supports between MGs [2]. Considering the volatility, variability, and uncertainty of renewable energies as well as the complicated dynamics of the inverter-based distributed energy resources (DERs), it is of critical significance to study the transient stability of the NMG with high penetration of DERs.

Microgrid transient stability investigates whether the system recovers to a steady state which satisfies operational constraints after a major disturbance [3]. Transient stability simulations can either be performed in a centralized or distributed manner while the centralized algorithms have been the focus of many studies from the perspectives of, e.g., microgrid dynamic modelling [4], dynamic response [5], impact of the DER control strategy [6], impact of the load type [7], etc. However, the centralized transient stability analysis of NMGs encounters two major obstacles: (1) the computational burden for solving large-scale differential algebraic equations (DAE) due to inverter-based DERs with complicated controllers embedded in an NMG and (2) privacy disclosure for microgrids of different owners.

In view of these limitations, the distributed transient stability (DTS) analysis emerges [8] for being capable of addressing the above issues. Several studies have discussed the DTS methodology for the bulk power system [9]-[12]. Usually, the states of boundary buses among different regions are employed for information exchange in the DTS calculation [9]. A DTS can be implemented based the distributed algorithms [10] with a decomposition of the dynamic model decomposition [11], [12]. Yet the following challenges have been recognized for the NMG applications of the DTS: (1) With high penetration of DERs, DTS should fully incorporate the controllers' dynamics; (2) With droop control of DERs, the system frequency is influenced by the dynamics of all the DERs in the distributed calculation; (3) Considering the "plug-and-play" feature in NMG operation, DTS should be flexible to accommodate the engagement/disengagement of a single MG at any time.

This paper focuses on the distributed transient stability of the networked microgrids. The main contributions are two-fold: 1) an ODE-based microgrid model is established to accurately capture the dynamics of the DER droop controllers as well as those of the loads and network; and 2) an ODE-enabled DTS methodology is devised for the NMGs, with special consideration of the frequency dynamics. Case studies are performed to verify the correctness and efficacy of the ODE-based microgrid model as well as the DTS method.

The remainder of this paper is organized as follows. Section II reviews the preliminary work in developing the DAE-based MG model. Section III presents the mathematical details of converting a DAE-model for a microgrid to its equivalent ODE counterpart. The ODE-based distributed transient stability method for the network microgrid (DTS-NMG) is developed in Section IV. Finally, a case study is discussed in Section V, followed by Conclusions.

II. Preliminaries

This section introduces the dynamic formulation of an islanded microgrid.

A DER controller with droop is considered, which employs the power controller, current controller and voltage controller:

$$\frac{\mathrm{d}\delta_i}{\mathrm{d}t} = \omega_i - \omega_{ref} \tag{1a}$$

$$\frac{\mathrm{d}P_i}{\mathrm{d}t} = \omega_{c,i}(-P_i + v_{od,i}i_{od,i} + v_{oq,i}i_{oq,i}) \tag{1b}$$

$$\frac{\mathrm{d}Q_i}{\mathrm{d}t} = \omega_{c,i}(-Q_i + v_{oq,i}i_{od,i} - v_{od,i}i_{oq,i}) \tag{1c}$$

This work was supported in part by the Department of Energy's Advanced Grid Modeling Program and in part by the National Science Foundation under Grant ECCS-1831811.

Y. Zhou and P. Zhang are with the Department of Electrical and Computer Engineering, Stony Brook University, NY 11794-2350, USA (e-mails: yifan.zhou.1@stonybrook.edu, p.zhang@stonybrook.edu).

M. Yue is with Brookhaven National Laboratory, , NY 11973-5000, USA (e-mail: yuemeng@bnl.gov).

978-1-7281-5508-1/20/$31.00 ©2020 IEEE

$$\frac{\mathrm{d}\phi_{dq,i}}{\mathrm{d}t} = v^*_{odq,i} - v_{odq,i} \tag{1d}$$

$$\frac{\mathrm{d}\gamma_{dq,i}}{\mathrm{d}t} = i^*_{Ldq,i} - i_{Ldq,i} \tag{1e}$$

$$\frac{\mathrm{d}i_{Ldq,i}}{\mathrm{d}t} = \frac{-r_{f,i}}{L_{f,i}} i_{Ldq,i} \pm \omega_i i_{Lqd,i} + \frac{1}{L_{f,i}}(v^*_{idq,i} - v_{odq,i}) \tag{1f}$$

$$\frac{\mathrm{d}v_{odq,i}}{\mathrm{d}t} = \pm\omega_i v_{oqd,i} + \frac{1}{C_{f,i}} i_{Ldq,i} - \frac{1}{C_{f,i}} i_{odq,i} \tag{1g}$$

$$\frac{\mathrm{d}i_{odq,i}}{\mathrm{d}t} = \frac{-r_{c,i}}{L_{c,i}} i_{odq,i} \pm \omega_i i_{oqd,i} + \frac{1}{L_{c,i}}(v_{odq,i} - v_{ndq,i}) \tag{1h}$$

where i denotes the DER index; t denotes the time. State variables of (1) include δ_i (DER angle), P_i (active power generation), Q_i (reactive power generation), $\phi_{dq,i} = [\phi_{d,i}; \phi_{q,i}]$ (output signal of the voltage controller in dq-axis), $\gamma_{dq,i} = [\gamma_{d,i}; \gamma_{q,i}]$ (output signal of the current controller in dq-axis), $i_{Ldq,i} = [i_{Ld,i}; i_{Lq,i}]$ (current after the output LC filter), $v_{odq,i} = [v_{od,i}; v_{oq,i}]$ (voltage output of DER in dq-axis), $i_{odq,i} = [i_{od,i}; i_{oq,i}]$ (current output of DER in dq-axis).

The nonlinear ODE in (1) formulates the dynamics of the droop controlled inverters, and this controller sketch is widely utilized to study the system transient responses under large disturbances [13], [14], [15]. Specifically, (1a)-(1c) formulate the power controller, where $\omega_i = \omega_{0,i} - m_{p,i}(P_i - P_{0,i})$ is the angular frequency; $m_{p,i}$ is the active power droop gain of DER i; $\omega_{0,i}$ is the nominal angular frequency; $P_{0,i}$ is the reference active power; ω_{ref} denotes the angular frequency of the reference DER [4]; $\omega_{c,i}$ is the filter parameter. Equation (1d) formulates the voltage controller, where $v^*_{od,i} = V_{n,i} - n_{q,i}Q_i$; $v^*_{oq,i} = 0$; $n_{q,i}$ is the reactive power droop gain of DER i; $V_{n,i}$ is the nominal voltage parameter. Equation (1e) formulates the current controller, where $i^*_{Ldq,i} = F_i i_{odq,i} \mp \omega_{n,i} C_{f,i} v_{oqd,i} + K_{pv,i}(v^*_{odq,i} - v_{odq,i}) + K_{iv,i}\phi_{dq,i}$; and F_i, $K_{pv,i}$, $K_{iv,i}$, $C_{f,i}$ are controller parameters. Equations (1f)-(1h) models the LC filter for DER voltage and current output, where $v^*_{idq,i} = \mp\omega_{n,i} L_{f,i} i_{Lqd,i} + K_{pc,i}(i^*_{Ldq,i} - i_{Ldq,i}) + K_{ic,i}\gamma_{dq,i}$; and F_i, $K_{pc,i}$, $K_{ic,i}$, $L_{f,i}$ are controller parameters; $v_{nd,i}$ and $v_{nq,i}$ are dq-axis voltage at the bus connected to DER i.

Recently, it has been reported that neglecting the dynamics in power lines and loads leads to overly optimistic stability assessment. This motivated us to model the dynamics in the entire NMG. For each constant impedance load, the dynamics are described by the load resistance and inductance:

$$\frac{\mathrm{d}i_{lDQ,j}}{\mathrm{d}t} = -\frac{r_{l,j}}{L_{l,j}} i_{lDQ,j} \pm \omega_{ref} i_{lQD,j} + \frac{1}{L_{l,j}} v_{lDQ,j} \tag{2}$$

where j denotes the load index; $i_{lDQ,j} = [i_{lD,j}; i_{lQ,j}]$ denotes the load current j in DQ-axis (*i.e.*, the common reference frame [4]); $v_{lDQ,j} = [v_{lD,j}; v_{lQ,j}]$ denotes the DQ-axis voltage at the bus connected to load j; $r_{l,j}$ and $L_{l,j}$ are the load resistance and inductance.

For each branch in the microgrid, the dynamics are modeled by the branch resistance and inductance:

$$\frac{\mathrm{d}i_{bDQ,k}}{\mathrm{d}t} = -\frac{r_{b,k}}{L_{b,k}} i_{bDQ,k} \pm \omega_{ref} i_{bQD,k} + \frac{1}{L_{b,k}} v_{bDQ,k} \tag{3}$$

where k denotes the branch index; $i_{bDQ,k} = [i_{bD,k}; i_{bQ,k}]$ denote the branch currents in DQ-axis; $v_{bDQ,k} = [v_{bD,k}; v_{bQ,k}]$ is the DQ-axis voltage difference along the branch; $r_{b,k}$ and $L_{b,k}$ are the branch resistance and inductance.

At each bus of the microgrid, the Kirchhoff's Current Law (KCL) should be satisfied:

$$0 = \sum_{i \in \mathcal{S}_n^{DER}} i_{oDQ,i} - \sum_{j \in \mathcal{S}_n^l} i_{lDQ,j} - \sum_{k \in \mathcal{S}_n^b} i_{bDQ,k} \tag{4}$$

where n is the bus index; $\mathcal{S}_n^{DER}$, $\mathcal{S}_n^l$ and $\mathcal{S}_n^b$ denote the sets of DERs, loads and branches connected to bus n; $i_{oDQ,i} = [i_{oD,i}; i_{oQ,i}]$ denotes the output current of DER i in the DQ-axis by the following transformation:

$$\begin{bmatrix} i_{oD,i} \\ i_{oQ,i} \end{bmatrix} = \begin{bmatrix} \cos\delta_i & -\sin\delta_i \\ \sin\delta_i & \cos\delta_i \end{bmatrix} \begin{bmatrix} i_{od,i} \\ i_{oq,i} \end{bmatrix} \tag{5}$$

By integrating (1)-(5), the microgrid model can be established, which is a nonlinear DAE model addressing the transient responses of each microgrid component. To solve it, the differential and algebraic equations should be interactively solved, which is complicated and time-consuming.

III. ODE-based Microgrid Model

In this section, a full ODE-based microgrid model (ODE-MG model) is devised by performing a rigorously equivalent conversion from DAE to ODE.

A. Basic Methodology for DAE-ODE Conversion

This subsection starts from a linear DAE-ODE conversion. The nonlinear case which addresses the nonlinearity nature of the microgrid dynamics will be handled in the next subsection. Consider a linear DAE model abstracted as:

$$\begin{cases} \dot{x} = Ax + By \\ Cx = 0 \end{cases} \tag{6}$$

where x is a m-dimensional vector of the differential variables; y is a n-dimensional vector of the algebraic variables; $A_{m\times m}, B_{m\times n}, C_{n\times m}$ are parameter matrices.

We suppose that the following four conditions hold: (1) $m \geq n$; (2) A is non-singular; (3) B is column full rank; (4) C is row full rank. Otherwise, it can be proved that the redundant variables can be eliminated to satisfy these conditions.

Denote C_1 as the sub-matrix of C constructed by its m independent columns, and C_0 as the sub-matrix constructed by the other columns. Denote the elements of x corresponding to C_0 as x_0 and the others as x_1. Accordingly, (6) can be written as the following:

$$\begin{cases} \dot{x_0} = A_{00}x_0 + A_{01}x_1 + B_0 y \\ \dot{x_1} = A_{10}x_0 + A_{11}x_1 + B_1 y \\ C_0 x_0 + C_1 x_1 = 0 \end{cases} \tag{7}$$

where $A_{00}, A_{01}, A_{10}, A_{11}, B_0, B_1$ are sub-matrices of A or B by extracting the columns or rows corresponding to x_0 or x_1.

Obviously, C_1 is non-singular, which yields $x_1 = -C_1^{-1}C_0 x_0$. Substituting it into (7) leads to the following:

$$\begin{cases} \dot{x_0} = (A_{00} - A_{01}C_1^{-1}C_0)x_0 + B_0 y & \text{(8a)} \\ -C_0\dot{x_0} = C_1(A_{10} - A_{11}C_1^{-1}C_0)x_0 + C_1 B_1 y & \text{(8b)} \end{cases}$$

Left multiplying (8a) with C_0 and adding it to (8b) yields:

$$Mx_0 + Ny = 0 \tag{9}$$

where $M = \left[C_0(A_{00} - A_{01}C_1^{-1}C_0) + C_1(A_{10} - A_{11}C_1^{-1}C_0)\right]$; $N = C_0B_0 + C_1B_1 = CB$.

If N is non-singular, the algebraic variables y can be expressed by the differential variables x as $y = -N^{-1}Mx_0$. As a result, we obtain a $m-n$ dimensional ODE model that is rigorously equivalent to the original DAE model (6):

$$\dot{x_0} = (A_{00} - A_{01}C_1^{-1}C_0 - B_0N^{-1}M)x_0 \tag{10}$$

If N is singular, (6) degenerates to an equivalent DAE model with a lower order. Hence, above conversion can still be implemented.

B. DAE-ODE Conversion of Microgrid Model

The conversion from the nonlinear microgrid DAE model to a nonlinear ODE is delineated here.

Denote $\mathbf{i}_{oDQ}$ as the vector form of $i_{oD,i}$ and $i_{oQ,i}$ for all the DERs. In analogy, denote $\mathbf{i}_{lDQ}$ for the loads, and $\mathbf{i}_{bDQ}$ for the branches. We can rewrite the output current equations of each DER (1h) as well as the dynamics of loads and branches (2)-(3) into a matrix form:

$$\begin{aligned}
\mathbf{L}_c\frac{\mathrm{d}\mathbf{i}_{oDQ}}{\mathrm{d}t} &= -\mathbf{r}_c\mathbf{i}_{oDQ} \pm \omega_{ref}\mathbf{L}_c\mathbf{i}_{oQD} + \mathbf{v}_{oDQ} - \mathbf{M}_g\mathbf{v}_{nDQ}\\
\mathbf{L}_l\frac{\mathrm{d}\mathbf{i}_{lDQ}}{\mathrm{d}t} &= -\mathbf{r}_l\mathbf{i}_{lDQ} \pm \omega_{ref}\mathbf{L}_l\mathbf{i}_{lQD} + \mathbf{M}_l\mathbf{v}_{nDQ}\\
\mathbf{L}_b\frac{\mathrm{d}\mathbf{i}_{bDQ}}{\mathrm{d}t} &= -\mathbf{r}_b\mathbf{i}_{bDQ} \pm \omega_{ref}\mathbf{L}_b\mathbf{i}_{bQD} + \mathbf{M}_b\mathbf{v}_{nDQ}
\end{aligned} \tag{11}$$

where $\mathbf{v}_{oDQ}$ is the vector form of DER output voltages in the DQ-axis; $\mathbf{v}_{nDQ}$ is the vector form of DQ-axis bus voltages; $\mathbf{M}_g$ is the incidence matrix between DER and bus, which contains 1 when DER i is at bus s, and 0 otherwise; $\mathbf{M}_l$ and $\mathbf{M}_b$ are incidence matrices between load/branch and bus defined similarly; $\mathbf{L_c}$ is a diagonal matrix with $L_{c,i}$ as the diagonal element, and $\mathbf{r_c}$, $\mathbf{L_l}$, $\mathbf{r_l}$, $\mathbf{r_b}$, $\mathbf{r_b}$ are defined similarly.

The matrix-form KCL equation can be written as follows:

$$\mathbf{M}_g^T\mathbf{i}_{oDQ} - \mathbf{M}_l^T\mathbf{i}_{lDQ} - \mathbf{M}_b^T\mathbf{i}_{bDQ} = \mathbf{0} \tag{12}$$

Denote $x = [\mathbf{i}_{oDQ}; \mathbf{i}_{lDQ}; \mathbf{i}_{bDQ}]$ as the vector of differential variables, and $y = \mathbf{v}_{nDQ}$ as the vector of algebraic variables. Denote z as the vector of other state variables in the microgrid model. Accordingly, the microgrid model formulated by (1a)-(1g), (11) and (12) is abstracted as:

$$\begin{cases}
\dot{z} = f(x,z)\\
\dot{x} = Ax + By + g(x,z)\\
Cx = 0
\end{cases} \tag{13}$$

where the expression of A, B, C, f and g can be readily obtained from the microgrid model. Due to page limitation, the details are omitted.

Following the derivations in subsection III-A, the above DAE can be equivalently converted to an ODE model as:

$$\begin{cases}
\dot{z} = \hat{f}(x_0,z)\\
\dot{x_0} = (A_{00} - A_{01}C_1^{-1}C_0 - B_0N^{-1}M)x_0\\
\qquad\quad - B_0N^{-1}C\hat{g}(x_0,z) + \hat{g}_0(x_0,z)
\end{cases} \tag{14}$$

where $\hat{f}(x_0,z) = f(x_0,x_1,z)$; $\hat{g}(x_0,z) = g(x_0,x_1,z)$; $\hat{g}_0$ extracts the elements of $\hat{g}$ corresponding to x_0. It should be noted that for the microgrid model, A in (13) is not a constant matrix (*i.e.*, ω_{ref} is involved). Hence, its sub-matrices (*i.e.*, $A_{00}, A_{01}, A_{10}, A_{11}$) are also time-varying matrices and should be updated in each time step in the transient simulation.

By appropriately choosing the sub-matrix of C, the DAE-ODE conversion can be performed. To avoid complicated reformulation of the DER model, it is recommended to reserve $\mathbf{i}_{oD}$ and $\mathbf{i}_{oQ}$ in x_0. The main computational effort for DAE-ODE conversion is related to the inverse of C_1 and N. However, since they are constant matrices, the inverse computation is performed only once before the transient stability analysis.

The advantages of the ODE-MG model can be summarized as the following:

(a) **Equivalent**: ODE-MG is strictly equivalent to the original DAE model since the DAE-ODE conversion is rigorous.

(b) **Concise**: Considering the sparsity feature of the power grid, the scale of the ODE-MG model mainly depends on the number of the DERs and power loads.

(c) **Efficient**: Solving the ODE model is much more efficient than solving the DAE model.

(d) **Adaptive**: The DAE-ODE conversion is independent to the internal model of the DER controller. Hence, it can readily accommodate various control strategy of the DERs.

Additionally, the DAE-ODE conversion can readily incorporate the synchronous generators by taking the dynamic of the DQ-axis outflow currents into (11) and (12). Due to the page limit, details of the generator dynamics are not presented.

IV. Distributed Transient Stability in Networked Microgrid

A networked microgrid integrates multiple small-scale microgrids to a backbone network via the points of common coupling (PCCs). Using the ODE-MG model, this section devises a distributed transient stability (DTS) algorithm for the NMG (DTS-NMG algorithm), which fully considers the dynamics of the DERs as well as the privacy of each MG.

A. DTS-NMG Algorithm Outline

The interface states between each microgrid and the backbone network include: (a) the DQ-axis bus voltages (*i.e.*, v_{nD}, v_{nQ}) and branch currents (*i.e.*, i_{lD}, i_{lQ}) at the connection between the microgrid and the backbone network, which are denoted by V_{pcc} and I_{pcc} in Figure.1; (b) the system frequency (*i.e.*,ω_{ref}). The feature of the DTS scheme for NMG is that, both the boundary voltage/current and the system frequency, which is impacted by the dynamics of all the DERs in the NMG, will be matched in the distributed calculation. This feature can be further illustrated in Figure 1. The reference DER is assumed to be located in MG1. Designating the interface states between each microgrid and the backbone network as the DQ-axis voltages and currents (*i.e.*, V_{pcc},I_{pcc}) as well as the system frequency (ω_{ref}), the following steps are performed for iterations at each time step in the DTS-NMG until convergence:

Step 1 (transient of MG1): input of MG1 is the DQ-axis current injection at PCC, *i.e.*, I_{pcc1}; output includes the reference angular frequency (*i.e.*, ω_{ref}) and the DQ-axis voltage at PCC.

Step 2 (transient of the backbone grid): input includes the PCC voltage at MG1, PCC current from other MGs and the ω_{ref}; output includes the PCC voltage of other MGs.

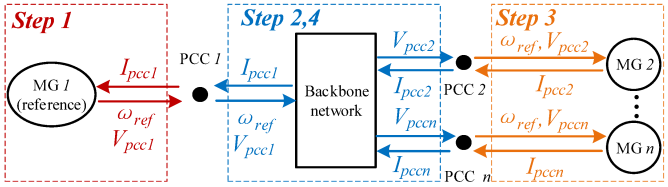

Fig. 1. Outline of distributed transient stability of NMG (DTS-NMG)

Step 3 (transient of other MGs): input includes the PCC voltage and ω_{ref}; output is the current injection to each MG.

Step 4 (transient of the backbone grid): input includes the PCC voltage at MG1, PCC current from other MGs and the ω_{ref}; output is the current injection to MG1.

The DTS-NMG method has the following advantages:

(a) **Parallelizable**: The large-scale ODE model of the NMG is decomposed into a set of small-scale ODE models which can be calculated in parallel to make the DTS more efficient.

(b) **Flexible**: When a single MG joins or quits the NMG, only the boundary conditions for the backbone network need to be modified at the specific PCC when applying the DTS-NMG algorithm, without impacting the transient stability analyses in other MGs, *i.e.*, the "plug-and-play" feature of the NMG.

(c) **Private**: The transient analysis for each MG is performed individually and independently, which better preserves the privacy of each MG.

B. ODE-MG Model With Boundary Conditions

In the DTS-NMG algorithm designed above, the dynamics of each MG are calculated with a specific boundary condition (*i.e.*, bus voltage or current injection). Similar to (6), for an MG with certain boundary conditions, its dynamic model can be abstracted as the following DAE:

$$\begin{cases} \dot{z} = f(x,z) \\ \dot{x} = Ax + By + g(x,z) + DV \\ Cx = EI \end{cases} \tag{15}$$

where V is the DQ-axis voltage at the boundary bus; I introduces the current injection at the boundary bus; D and E are parameter matrices. Specifically, for the PCC bus with given bus voltage, the corresponding KCL should be slack.

In analogy to the DAE-ODE conversion derived in section III-A, (15) can be finally reformulated as an ODE-model as:

$$\begin{cases} \dot{z} = \hat{f}(x_0,z) \\ \dot{x_0} = (A_{00} - A_{01}C_1^{-1}C_0 - B_0N^{-1}M)x_0 - B_0N^{-1}C\hat{g} + \hat{g}_0 \\ \qquad + (D_0 - B_0N^{-1}CD)V \\ \qquad + (A_{01}C_1^{-1} - B_0N^{-1}K)EI + B_0N^{-1}E\dot{I} \end{cases} \tag{16}$$

where D_0 is the sub-matrix of D by extracting the rows corresponding to x_0; $K = (C_0A_{01} + C_1A_{11})C_1^{-1}$.

V. Case Study

This section performs the case study. All the code is developed in MATLAB and runs on a 2.50GHz PC.

A. Validity of the ODE-MG Model

A simulation is conducted for the MG with 3 DERs, 2 power loads and 2 branches [4]. The proposed ODE-MG model and an ODE-based MG model presented in [4] are compared;

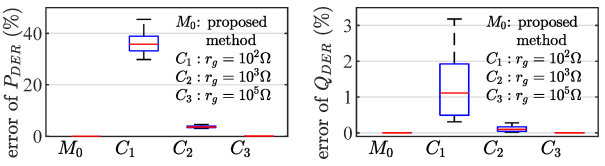

(a) DER active power generation (b) DER reactive power generation

Fig. 2. Relative error comparison of the steady-state operation point between the ODE-MG model and model in [4]

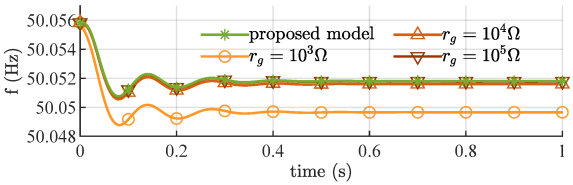

(a) system frequency

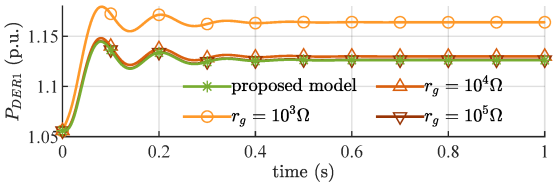

(b) active power generation of DER1

Fig. 3. Dynamic response comparison between ODE-MG model and model in [4] with different r_g

the latter is widely utilized by introducing a sufficiently large virtual resistance r_g to approximate the bus voltage:

$$v_{nD} = r_g\Big(\sum_{i\in\mathcal{S}_n^{DER}} i_{oD,i} - \sum_{j\in\mathcal{S}_n^{l}} i_{lD,j} - \sum_{k\in\mathcal{S}_n^{b}} i_{bD,k}\Big)$$

Figure 2 presents the relative error of the steady-state solution solved by the proposed ODE-MG model and the model in [4] with different r_g. P_{DER} and Q_{DER} separately denote the active and reactive power generation of each DER. The steady-state solution directly solved by the DAE-base microgrid model is taken as the base case. 50 scenarios are generated with uncertain output from the renewable energies. Simulation results indicate that the ODE-MG model precisely obtains the steady operating point of the dynamic system. In contrast, since [4] presents an approximation of the algebraic equations with the virtual resistance, it requires at least $r_g > 10^5$ to get a precise enough solution. Further, Figure 3 presents the comparison of the dynamic responses. The proposed ODE-MG model also matches well with the base case transients while the transient trajectory by [4] does not reflect the real dynamic process of the MG if r_g is not large enough.

Although satisfactory results can be obtained by setting a

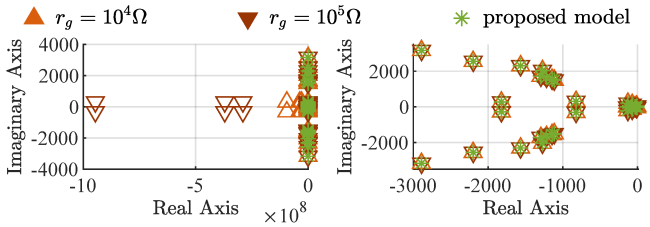

(a) numerical eigenvalues (b) eigenvalues reflecting the real dynamic characteristics

Fig. 4. Eigenvalue comparison between ODE-MG model and model in [4]

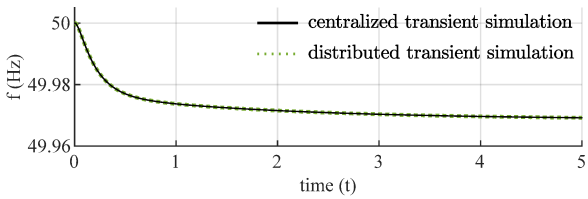

(a) transient trajectory with a 20% step of power load 1

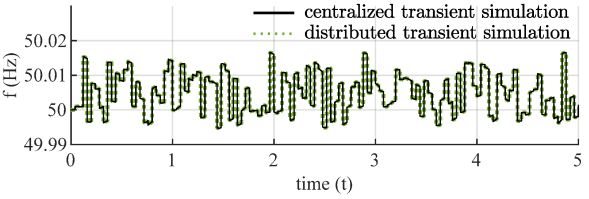

(b) transient trajectory with fluctuating renewable energy output

Fig. 5. Transient trajectory comparison between the centralized and distributed transient simulation

large enough r_g, it leads to bad numerical stability of the microgrid model. Fig.4 shows that the virtual resistance introduces eigenvalues with enormous negative real part. Although these eigenvalues correspond to the extremely fast modes and hence may not affect the system dynamic performance, they greatly deteriorate the numerical stability in the integral calculation. The proposed ODE-MG model, as a rigorous DAE equivalent, always reflects the inherent attributes of the MG system without introducing any additional "virtual" dynamics.

B. Validity of the DTS-NMG Method

A simulation is conducted using a NMG with 3 MGs, 5 DERs, 1 synchronous generator, 6 power loads and 9 branches. Figure 5 presents the transient stability results by both the centralized algorithm (*i.e.*, by directly integrating the NMG model) and the devised DTS-NMG algorithm. Two scenarios are considered. Firstly, Figure 5(a) demonstrates the ability of the DTS-NMG algorithm to follow the large disturbance. With a 20% step-change of power load 1, the system frequency drops and reaches a new steady state at 3s due to the dynamic of all the DERs. Simulation results show that the DTS-NMG algorithm matches well with the centralized transient stability results, for both the transient process and the new steady state. Secondly, Figure 5(b) demonstrates the ability of the DTS-NMG algorithm to follow the frequent disturbances. With 10% uncertainty of the renewable energy power, the system frequency fluctuates. Simulation results show that the DTS-NMG algorithm precisely follows this rapid dynamic process.

Figure 6 illustrates the iteration process of DTS-NMG in a single time step. As the iterations continue, MGs interact with each other via the boundary conditions at the PCCs. When the iterations stop, the states of each MG are the same as those in the centralized simulation.

VI. Conclusion

This paper establishes an ODE-based microgrid (ODE-MG) model to capture the dynamics in DERs, power loads and network with satisfactory numerical stability and computational efficiency. Using the ODE-MG model, a fully distributed

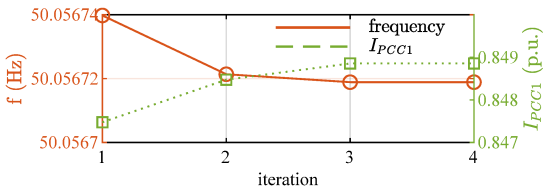

Fig. 6. Iteration between microgrids in a single time step

transient simulation (DTS) algorithm is devised for NMGs emphasizing on the frequency dynamics and the flexible "plug-and-play" feature of MGs. Numerical simulation verifies the validity of the ODE-MG model and the effectiveness of the DTS-NMG algorithm for scenarios of the single large disturbance and the frequently recurrent disturbances.

For future work, more delicate control (such as secondary control) and protection strategies (such as low-voltage ride through, low-frequency load shedding) will be incorporated in the DTS-NMG algorithm.

References

[1] R. H. Lasseter and P. Piagi, "Microgrid: A conceptual solution," in *IEEE Power Electronics Specialists Conference*, vol. 6, pp. 4285–4291, Citeseer, 2004.

[2] Z. Wang, B. Chen, J. Wang, and C. Chen, "Networked microgrids for self-healing power systems," *IEEE Transactions on Smart Grid*, vol. 7, no. 1, pp. 310–319, 2015.

[3] M. Farrokhabadi, C. A. Canizares, J. W. Simpson-Porco, E. Nasr, L. Fan, P. Mendoza-Araya, R. Tonkoski, U. Tamrakar, N. D. Hatziargyriou, D. Lagos, *et al.*, "Microgrid stability definitions, analysis, and examples," *IEEE Transactions on Power Systems*, 2019.

[4] N. Pogaku, M. Prodanovic, and T. C. Green, "Modeling, analysis and testing of autonomous operation of an inverter-based microgrid," *IEEE Transactions on Power Electronics*, vol. 22, no. 2, pp. 613–625, 2007.

[5] Y. Zhang and L. Xie, "A transient stability assessment framework in power electronic-interfaced distribution systems," *IEEE Transactions on Power Systems*, vol. 31, no. 6, pp. 5106–5114, 2016.

[6] M. Yu, W. Huang, N. Tai, X. Zheng, P. Wu, and W. Chen, "Transient stability mechanism of grid-connected inverter-interfaced distributed generators using droop control strategy," *Applied Energy*, vol. 210, pp. 737–747, 2018.

[7] N. Bottrell, M. Prodanovic, and T. C. Green, "Dynamic stability of a microgrid with an active load," *IEEE Transactions on Power Electronics*, vol. 28, no. 11, pp. 5107–5119, 2013.

[8] G. Aloisio, M. Bochicchio, M. La Scala, and R. Sbrizzai, "A distributed computing approach for real-time transient stability analysis," *IEEE Transactions on Power Systems*, vol. 12, no. 2, pp. 981–987, 1997.

[9] Y. Chen, C. Shen, and J. Wang, "Distributed transient stability simulation of power systems based on a jacobian-free newton-gmres method," *IEEE Transactions on Power Systems*, vol. 24, no. 1, pp. 146–156, 2009.

[10] S. Huang, Y. Chen, C. Shen, W. Xue, and J. Wang, "Feasibility study on online dsa through distributed time domain simulations in wan," *IEEE Transactions on Power Systems*, vol. 27, no. 3, pp. 1214–1224, 2012.

[11] P. Aristidou, S. Lebeau, and T. Van Cutsem, "Power system dynamic simulations using a parallel two-level schur-complement decomposition," *IEEE Transactions on Power Systems*, vol. 31, no. 5, pp. 3984–3995, 2015.

[12] S. Zadkhast, J. Jatskevich, and E. Vaahedi, "A multi-decomposition approach for accelerated time-domain simulation of transient stability problems," *IEEE Transactions on Power Systems*, vol. 30, no. 5, pp. 2301–2311, 2014.

[13] M. Kabalan, P. Singh, and D. Niebur, "Nonlinear lyapunov stability analysis of seven models of a DC/AC droop controlled inverter connected to an infinite bus," *IEEE Transactions on Smart Grid*, vol. 10, no. 1, pp. 772–781, 2017.

[14] D. K. Dheer, N. Soni, and S. Doolla, "Improvement of small signal stability margin and transient response in inverter-dominated microgrids," *Sustainable Energy, Grids and Networks*, vol. 5, pp. 135–147, 2016.

[15] L. Huang, H. Xin, Z. Wang, L. Zhang, K. Wu, and J. Hu, "Transient stability analysis and control design of droop-controlled voltage source converters considering current limitation," *IEEE Transactions on Smart Grid*, vol. 10, no. 1, pp. 578–591, 2017.